Supporting Information

Ni-Derived Electronic/Ionic Engineering on NiSe/Ni@C for Ultrafast and Stable Sodium Storage

Haiwei Li[a, #], Weilong Zhang[a, #], Lei Wang[b], Hongping Li[c], Yanchen Fan[d], Xiaolong Yang[a], Hui Du[a], Yan Zhang[a], Zhuo Li[a*]

[a] *School of Chemistry and Chemical Engineering, State Key Laboratory of Bio-fibers and Eco-textiles, Shandong Collaborative Innovation Center of Marine Biobased Fibers and Ecological Textiles, Qingdao University, Qingdao 266071, China*

b Institute of Materials for Energy and Environment, School of Materials Science and Engineering, Qingdao University, Qingdao, 266071 China

c School of Materials Science and Engineering, Suzhou University of Science and Technology, Suzhou 215011, China

d Petro China Shenzhen New Energy Research Institute, Shenzhen 518000, China

* Corresponding author: Zhuo Li (lizhuo831004@qdu.edu.cn)

[#] These authors contributed equally to this work.

1. Methods

1.1 Materials Synthesis: In a typical procedure, 10 g $Ni(NO_3)_2 \cdot 6H_2O$, 12 g citric acid and 2 g water-soluble starch were dissolved in deionized water to obtain a uniform and transparent solution and then transformed into a spray dryer. Then the precursor was carbonized at 500 ℃ for 1h under 10% H_2/Ar atmosphere to obtain the Ni@C precursor. Subsequently, the selenium vapor was introduced into the quartz-tube reactor at 700 ℃ for 2 h under 10% H_2/Ar atmosphere to prepare the NiSe/Ni@C.

1.2 Material Characterizations: The phase crystal of materials was characterized by X-ray diffraction (XRD) on Rigaku D/max-3C X-ray diffractometer with Cu Kα. Raman spectra was tested on a Renishaw in Via micro-Raman spectroscopy system with a laser wavelength of 780 nm. The micromorphology was characterized by a HELIOS NanoLab 600i field emission scanning electron microscope (FE-SEM). Transmission electron microscopy (TEM) and high-resolution TEM (HRTEM) of the samples were performed on JOEL JEM-2100F, Japan. X-ray photoelectron spectroscopy (XPS) was accomplished using a Thermo Scientific ESCALAB 250Xi X-ray photoelectron spectrometer. N_2 physical adsorption/desorption isotherms were achieved at -196 °C on an ASAP-2460-4HD apparatus. The carbon content was determined by Thermogravimetric Analysis (TG), TGA/DSC3$^+$, Mattler Toledo.

1.3 Electrochemical Measurements: The electrochemical evaluation was performed using 2032-type coin cells. The electrode was prepared by mixing active material, Super P and CMC in a weight ratio of 8:1:1. The slurry of the mixture was stirred for 12 h and then pasted on copper foil, and dried at 90°C for 12 h. Coin cells

were assembled using Na metal as reference electrode, $NaPF_6$ (EC: DEC=1:1) as electrolyte. The mass loading of active materials was about 1 mg cm^{-2}. Charge/discharge performance at various current was tested by Land battery circulator. Cyclic voltammetry (CV) measurement was performed on CHI 660E electrochemical workstation between 0.1 and 3.0 V. Electrochemical impedance spectroscopy (EIS) was conducted on CHI660E at the range of $0.01-10^5$ Hz.

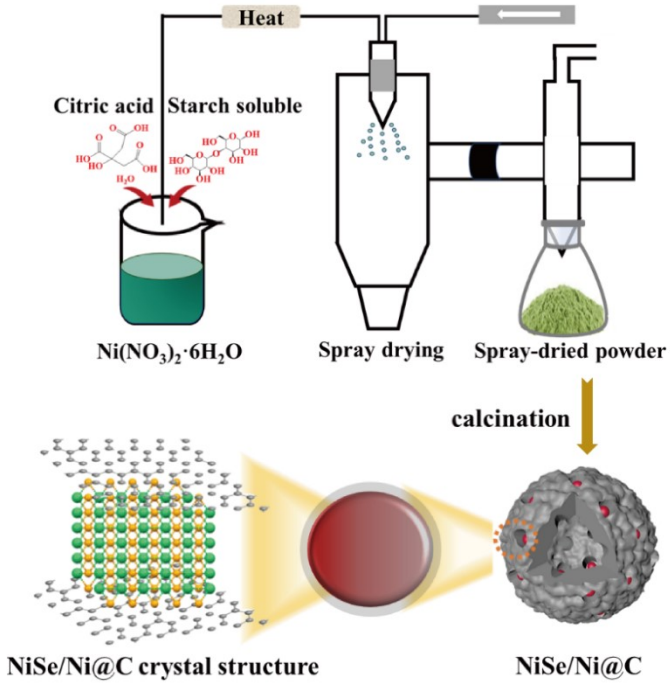

Figure S1. Schematic illustration of synthesis process of NiSe/Ni@C.

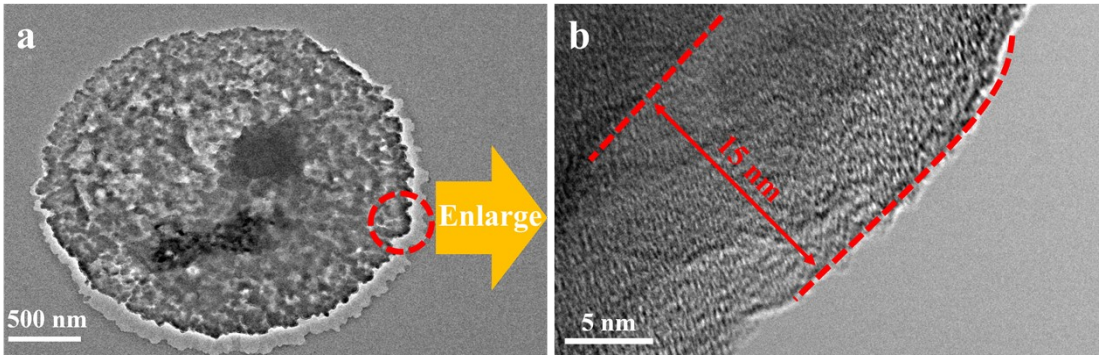

Figure S2. TEM images of NiSe/Ni@C a) at lower magnification, b) higher magnification (the red circle in (a))

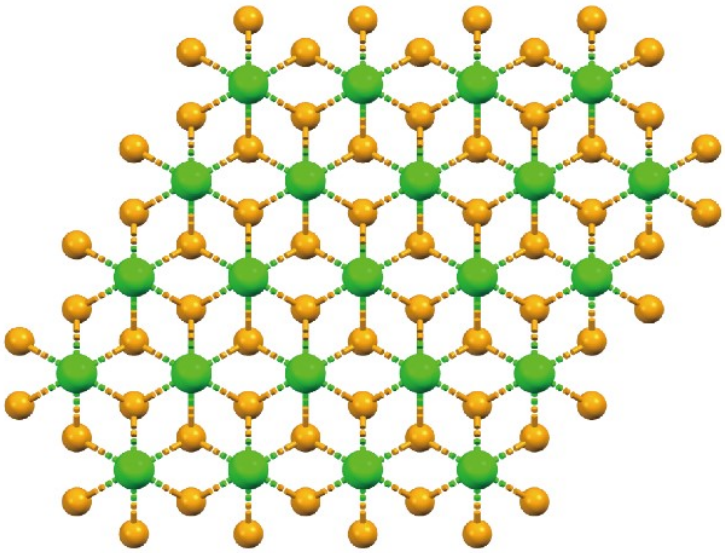

Figure S3. The ball and stick model of hexagonal-NiSe

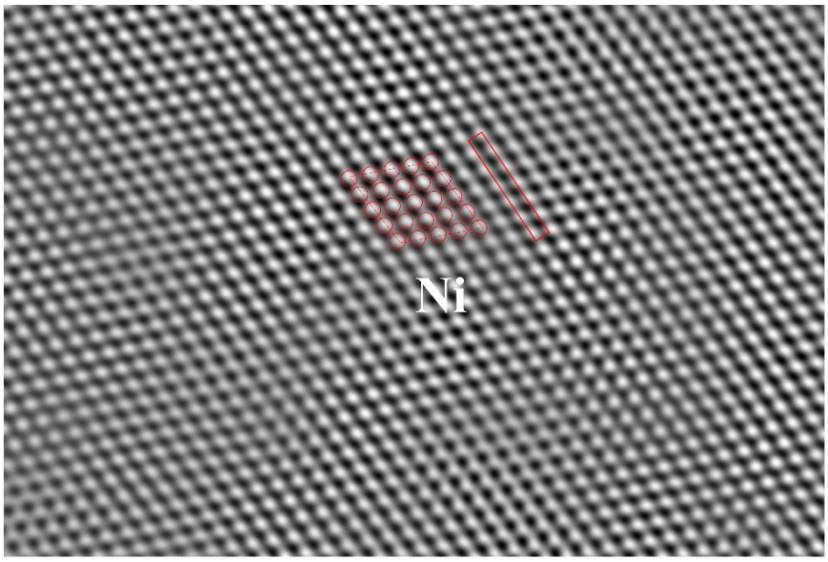

Figure S4. The inverse fast Fourier transformations of Ni

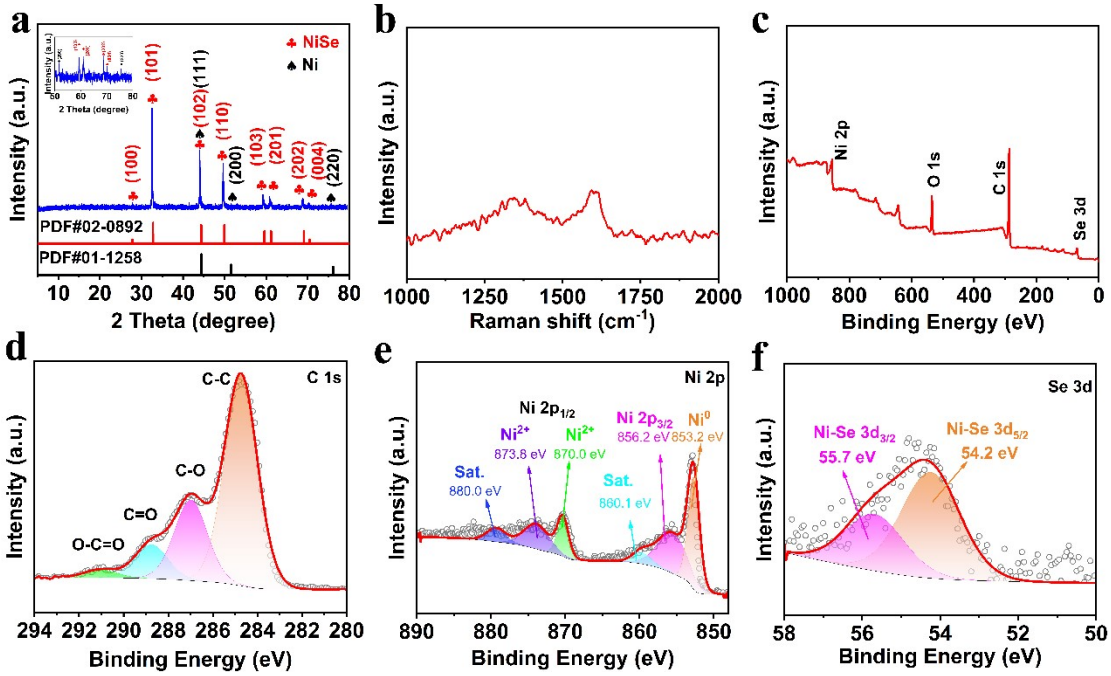

Figure S5. a) XRD pattern, b) Raman spectra, c) XPS survey, d-f) NiSe/Ni@C high-resolution XPS spectra (C 1s, Ni 2p, Se 3d).

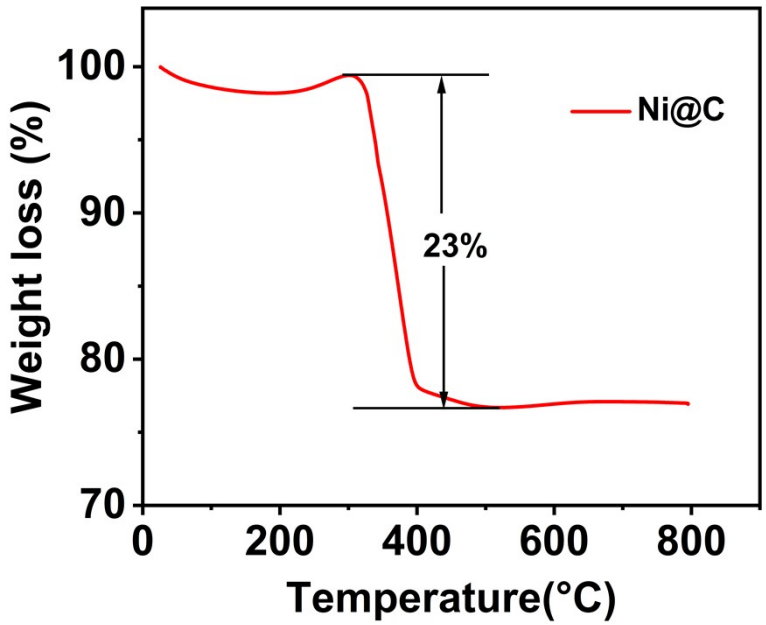

Figure S6. TG profile of Ni@C sample.

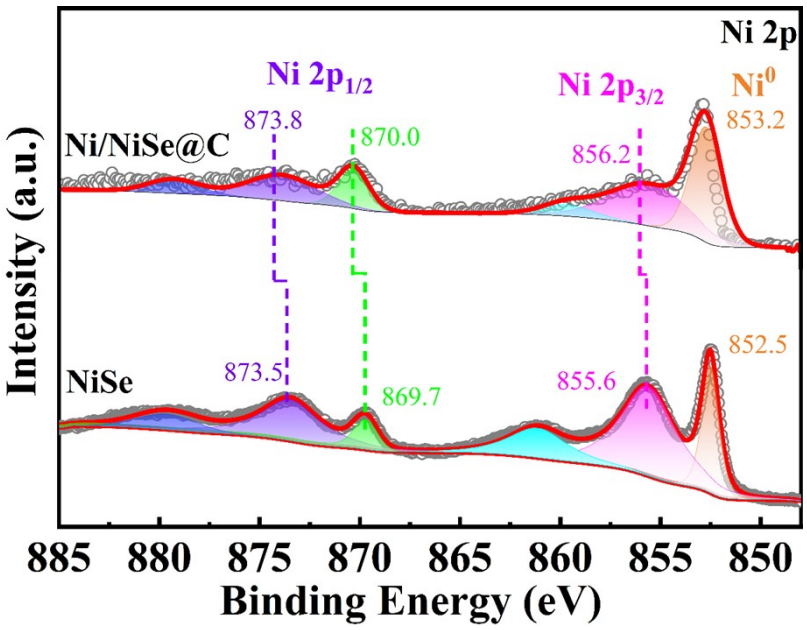

Figure S7. Ni 2p high-resolution XPS spectra of NiSe and NiSe/Ni@C.

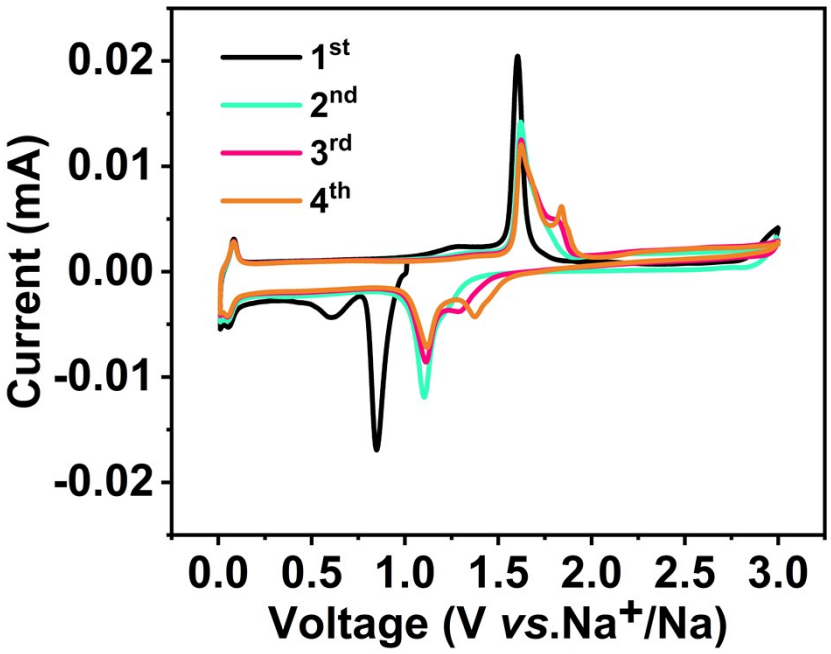

Figure S8. The CV curves of NiSe electrode (0.01 ~ 3.0 V at 0.1 mV s^{-1})

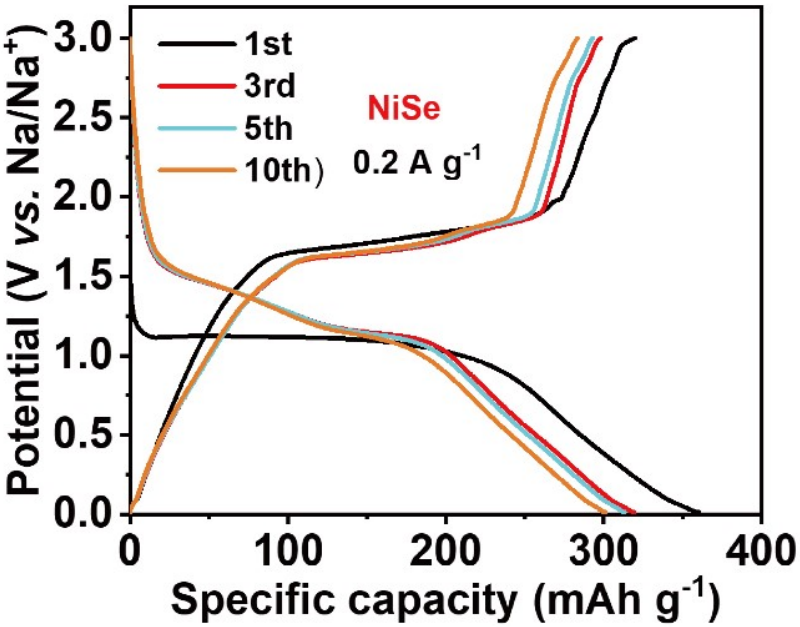

Figure S9. Charge/discharge profiles of NiSe at a current density of 0.2 A g^{-1}.

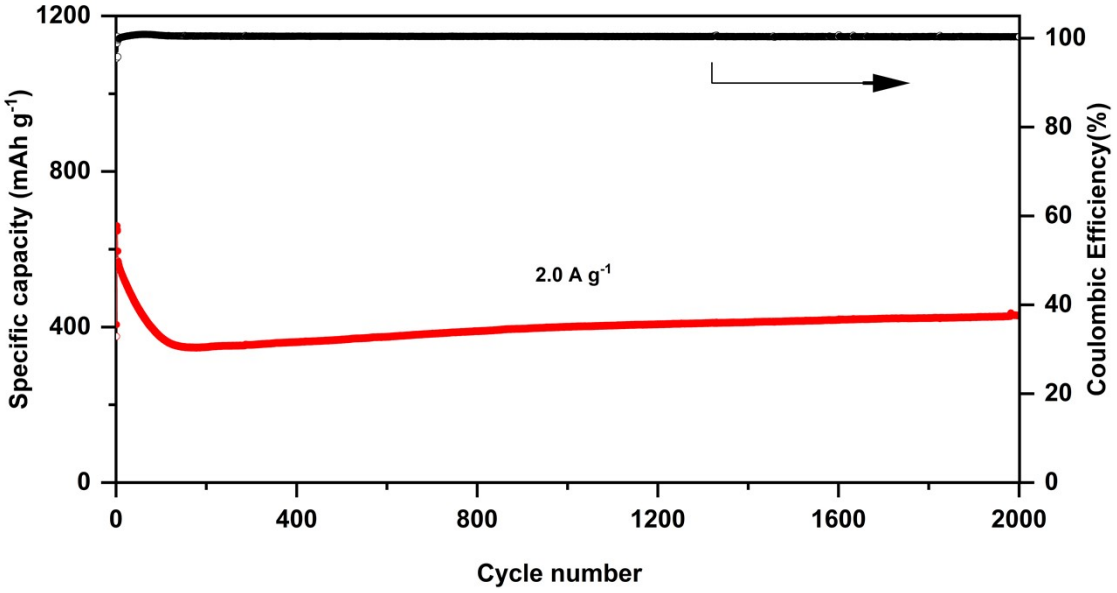

Figure S10. NiSe/Ni@C electrode cycling performance at 2.0 A g^{-1}.

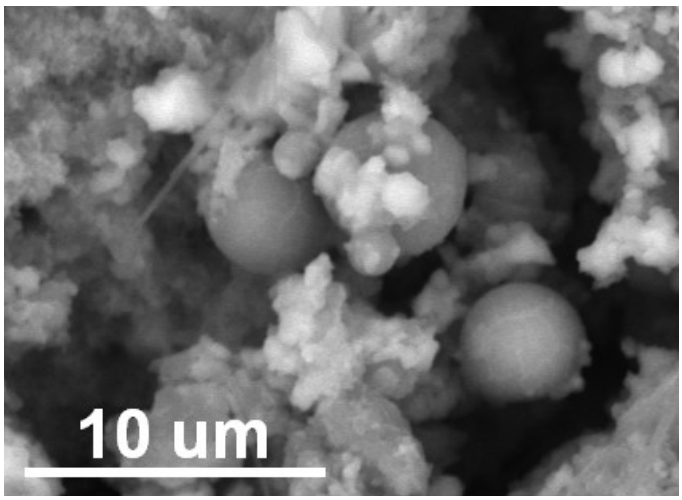

Figure S11. The cycled SEM of NiSe/Ni@C electrode at 1.0 A g^{-1}.

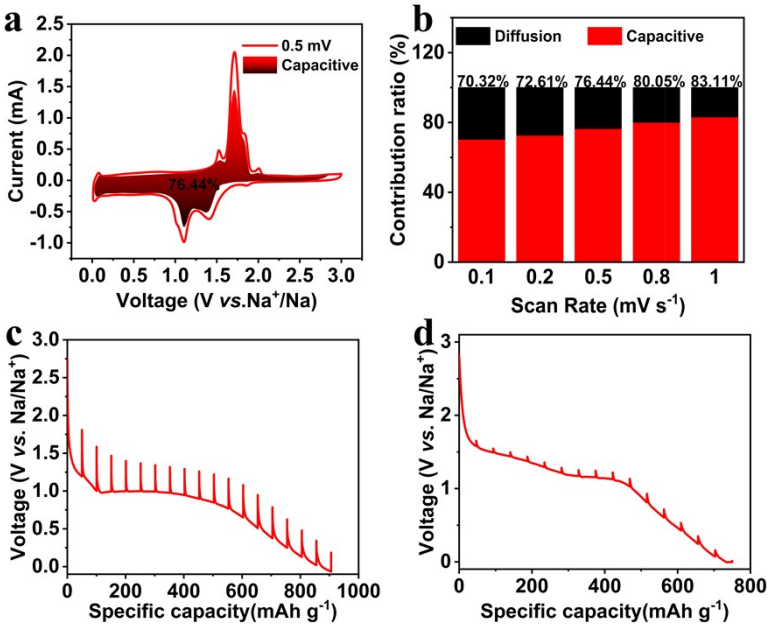

Figure S12. a) capacitive contribution at 0.5 mV s^{-1}. b) capacitive ratio at various scan rates. c) GITT profile of the NiSe/Ni@C, d) NiSe electrode.

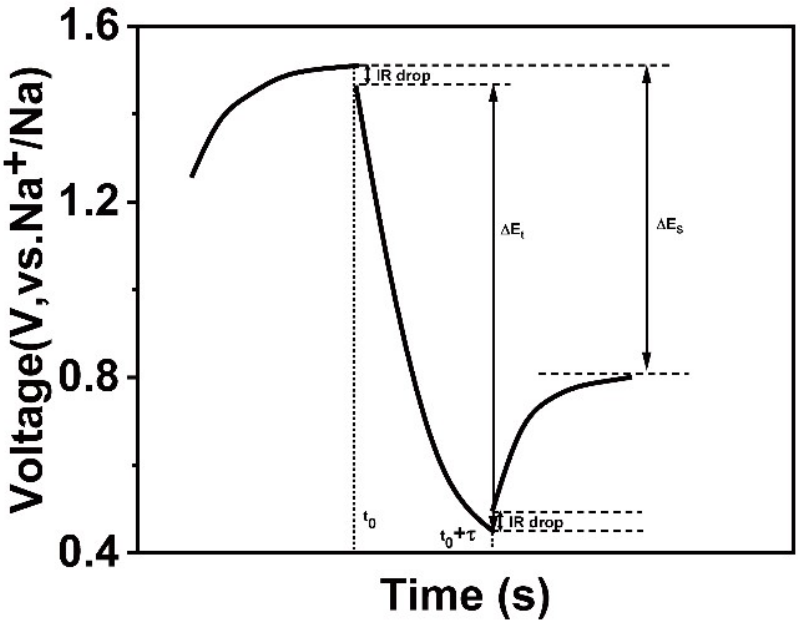

Figure S13. Schematic of GITT test

A series of D_{Na^+} were calculated at discharge process according to the following Eq. 1:

$$D_{Na^+} = \frac{4}{\pi}\left(\frac{m_B V_M}{M_B A}\right)^2\left(\frac{\Delta E_s}{\Delta E_t}\right)^2\left(\tau \ll \frac{L^2}{D_{Na^+}}\right) \quad \text{Eq. 1}$$

Where m_B (g) is the mass of the electrode, A (cm^2) is the surface area of the electrode, V_M (cm^3 mol^{-1}) is the molar volume of the electrode, M_B (g mol^{-1}) is the molecular weight, ΔEs (V) is the steady-state potential by the current pluse, L (cm) is the thickness of the electrode, ΔEt (V) is the change in potential during a constant current pulse after eliminating the iR drop.

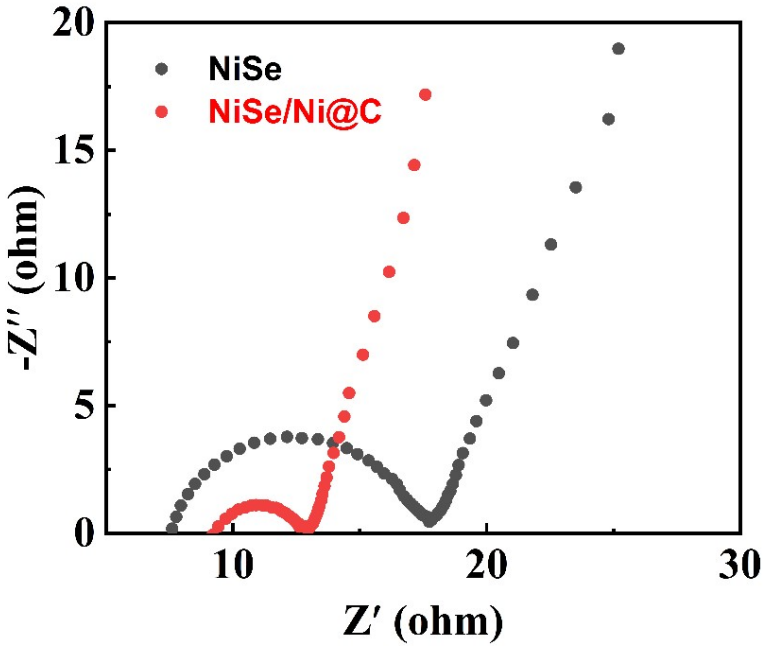

Figure S14. Nyquist plots of NiSe/Ni@C and NiSe electrodes after the cycling.

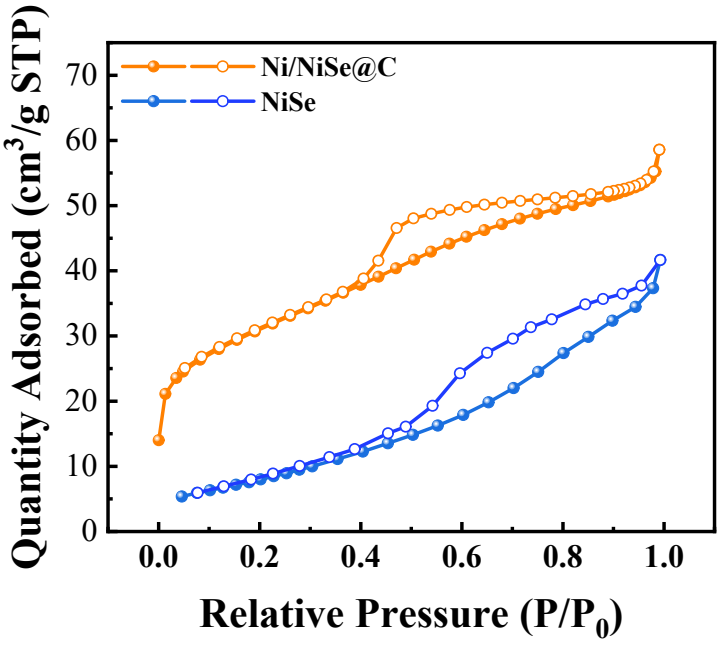

Figure S15. N_2 adsorption-desorption isotherms of NiSe/Ni@C and NiSe.

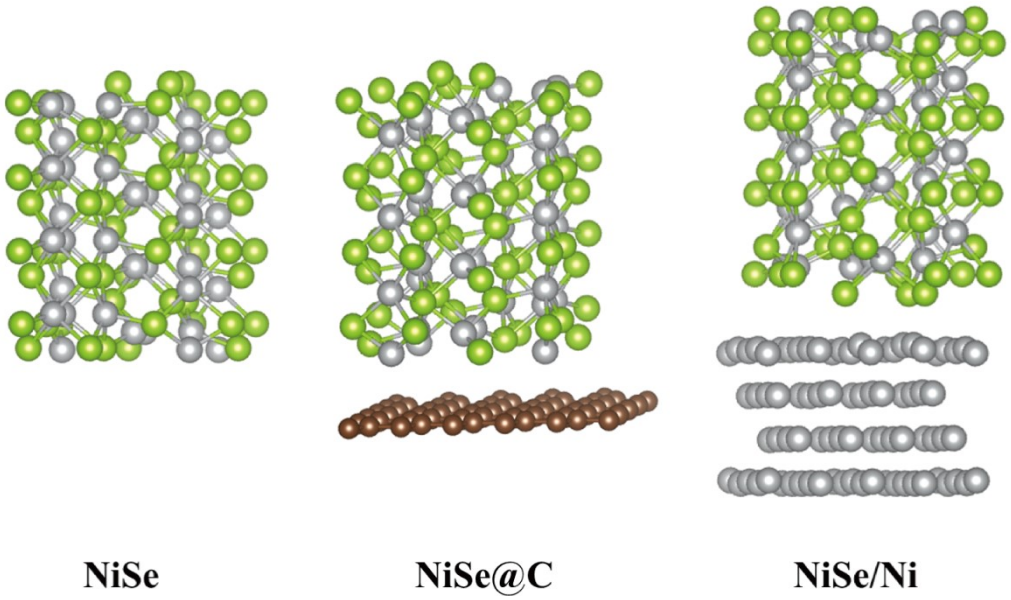

Figure S16. Structural models of NiSe, NiSe@C, and NiSe/Ni.

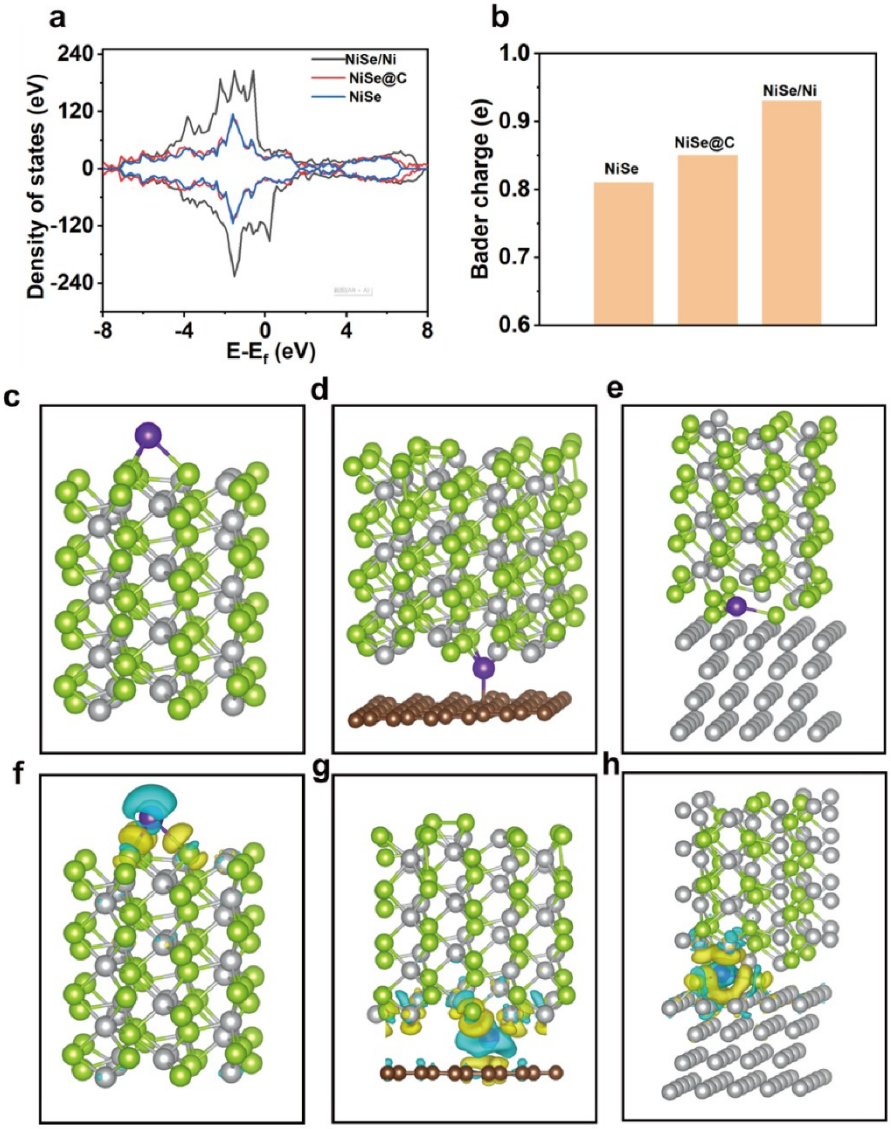

Figure S17. DFT calculation of the electrode. (a) the density of states (DOS), (b) bader charges of Na ion, (c-e) the adsorption energy diagrams of NiSe, NiSe@C, and NiSe/Ni, (f-h) the difference in charge density with Na adsorption at the interface.

Notes and references

1. T.T. Shan, S. Xin, Y. You, H.P. Cong, S.H. Yu and A. Manthiram, *Angew. Chem. Int. Ed.*, 2016, **55**, 12783-12788.
2. H. Kong, W. Cui, C. Yan, Y. Kong, C. Lv and G. Chen, *Chem. Eng. J.*, 2021, **419**, 129490.
3. C. Ma, Y. Hou, K. Jiang, L. Zhao, T. Olsen, Y. Fan, J. Jiang, Z. Xu, Z. Ma, D. Legut, H. Xiong and X.Z. Yuan, *Chem. Eng. J.*, 2021, **413**, 127449.
4. J. Qin, H. M. K. Sari, X. Wang, H. Yang, J. Zhang and X. Li, *Nano Energy*, 2020, **71**, 104594.
5. G. Li, B. Huang, Z. Pan, X. Su, Z. Shao and L. An, *Energy Environ. Sci.*, 2019, **12**, 2030-2053.
6. M. Á. Muñoz-Márquez, D. Saurel, J. L. Gómez-Cámer, M. Casas-Cabanas, E. Castillo-Martínez and T. Rojo, *Adv. Energy Mater.*, 2017, **7**, 1700463.
7. W. Zhao, X. Wang, X. Ma, L. Yue, Y. Ren, T. Li, J. Xia, L. Zhang, Q. Liu, Y. Luo, N. Li, B. Tang, Y. Liu, S. Gao, A. M. Asiri and X. Sun, *J. Mater. Chem. A.*, 2021, **9**, 27615-27628.
8. D. Zhao, R. Zhao, S. Dong, X. Miao, Z. Zhang, C. Wang and L. Yin, *Energy Environ. Sci.*, 2019, **12**, 2422-2432.
9. Z. Li, L. Zhang, X. Ge, C. Li, S. Dong, C. Wang and L. Yin, *Nano Energy*, 2017, **32**, 494-502.
10. Y. Fang, J. Zhang, L. Xiao, X. Ai, Y. Cao and H. Yang, *Adv. Sci.*, 2017, **4**, 1600392.

11. H. Xu, J. Fan, D. Pang, Y. Zheng, G. Chen, F. Du, Y. Gogotsi, Y. Dall'Agnese and Y. Gao, *Chem. Eng. J.*, 2022, **436**, 135012.

12. F. Zou, Y. M. Chen, K. Liu, Z. Yu, W. Liang, S. M. Bhaway, M. Gao and Y. Zhu, *ACS Nano*, 2016, **10**, 377-386.

13. Y. F. Zhu, Y. Xiao, W. B. Hua, S. Indris, S. X. Dou, Y. G. Guo and S. L. Chou, *Angew. Chem. Int. Ed.*, 2020, **59**, 9299-9304.

14. H. Fan, H. Yu, Y. Zhang, J. Guo, Z. Wang, H. Wang, N. Zhao, Y. Zheng, C. Du, Z. Dai, Q. Yan and J. Xu, *Energy Storage Mater.,* 2018, **10**, 48-55.

15. T. P. Gao, K. W. Wong and K. M. Ng, *Energy Storage Mater.,* 2020, **25**, 210-216.

16. Y. Fang, X. Y. Yu and X. W. Lou, *Adv. Mater.*, 2018, **30**, 1706668.

17. Z. Hao, X. Shi, Z. Yang, L. Li and S. L. Chou, *Adv. Funct. Mater.*, 2022, **32**, 2208093.

18. L. Sun, C. Wang and L. Wang, *ACS Nano*, 2018, **12**, 4002-4009.

19. E. Xu, Y. Zhang, H. Wang, Z. Zhu, J. Quan, Y. Chang, P. Li, D. Yu and Y. Jiang, *Chem. Eng. J.*, 2020, **385**, 123839.

20. Y. Zheng, T. Zhou, C. Zhang, J. Mao, H. Liu and Z. Guo, *Angew. Chem. Int. Ed.*, 2016, **55**, 3408-3413.

21. C. Guo, W. Zhang, Y. Liu, J. He, S. Yang, M. Liu, Q. Wang and Z. Guo, *Adv. Funct. Mater.*, 2019, **29**, 1901925.

22. D. Sun, K. Liu, J. Hu and J. Zhou, *Small*, 2021, **17**, 2006374.

23. E. Xu, Y. Zhang, H. Wang, Z. Zhu, J. Quan, Y. Chang, P. Li, D. Yu and Y. Jiang, Chem. Eng. J., 2020, 385, 123839.

24. X. Pu, D. Zhao, C. Fu, Z. Chen, S. Cao, C. Wang and Y. Cao, Angew. Chem. Int. Ed., 2021, 60, 21310-21318.
25. D. Chao, C. Zhu, P. Yang, X. Xia, J. Liu, J. Wang, X. Fan, S. V. Savilov, J. Lin, H. J. Fan and Z. X. Shen, Nat. Commun., 2016, 7, 12122.
26. W. Zhao, L. Gao, L. Yue, X. Wang, Q. Liu, Y. Luo, T. Li, X. Shi, A. M. Asiri and X. Sun, J. Mater. Chem. A, 2021, 9, 6402-6412.
27. C. Chen, Y. Wen, X. Hu, X. Ji, M. Yan, L. Mai, P. Hu, B. Shan and Y. Huang, Nat. Commun., 2015, 6, 6929.
28. J. Wang, J. Polleux, J. Lim and B. Dunn, J. Phys. Chem. C, 2007, 111, 14925-14931.